Building a Tensile Tester to Measure Single Silk Fibers

A senior team project report
submitted in partial fulfillment of the requirement for the degree of
Bachelor of Science in Physics,
Engineering Physics and Applied Design
from the College of William and Mary in Virginia,

by

Cody Hammack
Agustin O'Connell
Maya Leyden
Justin Dulaney
Jarice Mason, II
Thea Azzarone

_____
Mentor: Prof. Hannes Schniepp

_____
Prof. Jeffrey Nelson

Williamsburg, VA
April 30, 2020

1 Introduction

With global warming on the rise (Shankman and Horn 2019) and non-biodegradable plastics covering the earth (Lee 2019), the need for sustainable polymers is higher than ever (Pool 2019). Spider silk is an ideal alternative to non-biodegradable materials (Glover 2019) because it solely consists of proteins (Römer and Scheibel 2008). Not only is spider silk a natural fiber, but it is also known for its excellent structural properties (Römer and Scheibel 2008). Some spider silks have a specific strength that can be up to 5 times the specific strength of steel (MiceliNov 2018), and a specific toughness that is up to 3 times tougher than Kevlar (Römer and Scheibel 2008).The development of synthetic silk fibers could eventually replace other environmentally harmful fibers, but we first need to make sure that our synthetic silk is as strong as the naturally produced fibers.

In order to verify the mechanical properties of spider silk fibers, our team has been tasked with making a system for Professor Schniepp's lab that can measure the stress-strain curves of individual spider silk fibers, including the ribbon silk of the brown recluse spider. To accomplish this, we have worked with an MTS Criterion 42 (Eden Prairie, MN, http://mtsmonotonic.com/mts-criterion/) tensile tester (as shown in Fig. 1). At its base level, a tensile tester consists of two main components, a stage, and a load cell that measures the applied force on the sample. For our purposes, the stage of the Criterion 42 is good enough to stretch silk at a fixed rate. While silk has a high specific strength, single strands are very small and light, resulting in breaking forces on the order of 50 mN or less. The small forces involved means that the MTS load cells lack the needed sensitivity. Therefore, one of our goals was to find a load cell with suitable resolution, and successfully integrate it with the tensile tester. Additionally we wanted to create a repeatable process for mounting and testing silk strands to reduce the chances of tests being unsuccessful.

Figure 1: MTS Criterion Model 42 Tensile Tester.

Fundamentally, most load cells are strain gauges, which are read using a wheatstone bridge. A strain gauge is a device made by winding a conductive wire in a zigzag pattern such that it is effectively a long length of wire in a condensed space. When stretched, the wire becomes longer and thinner, increasing its resistance, which can then be measured. This allows the strain to be measured, and for a known gauge, this strain value can be converted into a force measurement.

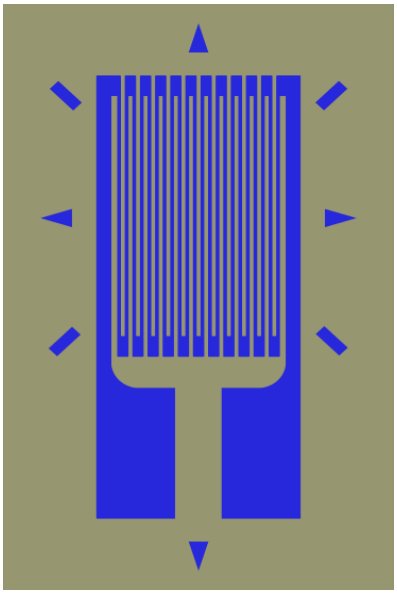

Figure 2: Strain Gauge.

A Wheatstone bridge is a type of circuit that allows for the resistance of an element to be measured with high accuracy. It consists of four resistors setup as shown in the image below.

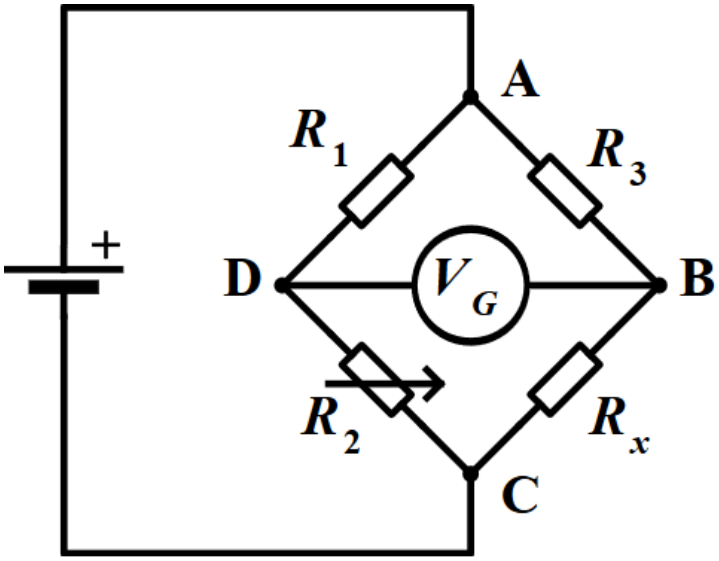

Figure 3: Wheatstone Bridge.

In the setup, R_1, R_2, and R_3 are all resistors of known values, and R_x is a resistor of unknown value, in our case the strain gauge. By sending in a known voltage, one can measure the voltage V_G, and using Kirchhoff's laws, find the resistance of R_x. In our case, knowing the resistance of R_x allows us to find the force applied to the strain gauge. With no applied force, all resistors are equal, resulting in V_G being equal to 0 V.

Most load cells have a rated output in mV/V, which is the ratio between the measured voltage and the applied voltage at the load cell's rated force. For forces below the rated force, the output is proportional to the amount of force compared to the rated force. This allows for the measured voltage to be converted into a force measurement. For example, For a 1N load cell with a rated output of 1 mV/V supplied with 10 V with 1 N applied, one would measure V_G to be 10 mV. If 0.1 N was applied, one would measure V_G to be 1 mV, which is one tenth of the output for one tenth of the force. For most load cells, the acceptable input voltages are in a range from about 5 V to 12 V, and the rated outputs are several mV/V. For load cells with a high resolution, such as ones rated Class 0.5, meaning they have sensitivity of 0.5% of the rated load, this can mean having to measure a signal on the order of microvolts.

With respect to the mechanical properties of spider silks, researchers are typically interested in their unique combination of high tensile strength and extensibility (ductility). This combination allows spider silk fibers to absorb large amounts of energy before breaking (Ko et al. 2018). Ability to absorb energy without breaking (work to fracture) is called toughness. Toughness is the area under the force x displacement curve divided by initial volume, where the area was only measured from the silk's first point of fracture.

A stress-strain curve graphically depicts the behavior of a material when it is subjected to a load (Asafar 2018). Stress is plotted vertically vs. Strain horizontally. From this relationship one can determine Yield Strength, Ultimate Strength, Fracture Point, Young's Modulus (from the slope), and toughness.

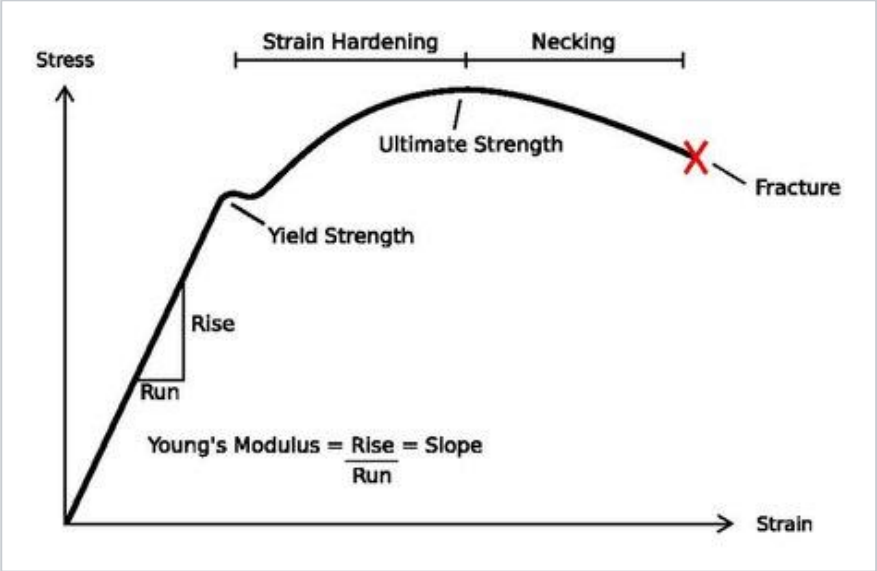

Figure 4: Stress-Strain Curve.

2 Specifications

Our specifications were determined by the physical properties of the silk we are testing. When defining our goals for resolution and maximum/minimum force requirements we looked at both orb weaver and brown recluse silk. The orb weaver's silk, along with most other silks, is cylindrical with a diameter on the order of 5 μm (Pérez-Rigueiro 2001). The brown recluse's silk is relatively unique in that it is more ribbon-like, with a width on the order of 5 μm, and a thickness on the order of tens of nanometers (Schniepp 2013). The small size of both types of silk meant that we needed some type of clamping mechanism that was gentle and small enough to hold on to the strands without damaging them or allowing them to slip.

The orb weaver's silk has a breaking force around 50 mN (Pérez-Rigueiro 2001) and the brown recluse's silk has a ribbon breaking force of about 300 μN (Wang and Schniepp 2018). With this knowledge the desired specifications for the load cell is a resolution on the order of 3 μN, which is 1% of the smallest breaking point, and will thus allow us to acquire a full stress–strain curve with a reasonable signal-to-noise ratio.

Load cells with the resolution we needed are designed for low amounts of force, and could break if too much force is applied. For example, the LSB 100 1N load cell (Irvine, CA) that came with the MTS Criterion 42 has a maximum force of 8 N. Therefore, the last requirement was devising a mounting technique that wouldn't pre-stress or overload the load cell. Heavy clamping devices used with the larger designated load cells are not applicable. Due to their large weight, attaching one to the 1N load cell would potentially damage it. Moving down an order of magnitude, a 0.1N load cell could be damaged simply by an errant pull. Thus a method of minimal force is required for attaching samples.

3 Engineering Design Options

3.1 Tensile Testing Apparatus

The MTS Criterion 42 is an electromechanical tensile tester, which is used for smaller force ranges compared to hydraulic systems. We also have three first-party load cells from them, a 1N, 100N, and 5kN (http://mtsmonotonic.com/accessories/). They are rated by the maximum force they can measure. and are each rated Class 0.5 from 1% to 100%. Class 0.5 is an accuracy class meaning that is accurate down to 0.5% of the rated load. Being rated Class 0.5 at 1% means it is accurate at 0.5% of 1% of the rated load, or 0.005% of the rated load. This means that the 1N load cell has a theoretical resolution of 50 μN, which is enough to measure larger silks, however it is insufficient for accurately measuring the brown recluse silk. Additionally, they have overload protection of up to 800% the rated loads. For our purposes, the tests themselves would

never reach the overload threshold, however for the 1N load cell, it could potentially exceed this protection during handling if caution was not taken.

We began searching for a new load cell to integrate with the Criterion 42 and settled on the F329 Deci-Newton load cell (http://micronewton.co.uk/loadcells.htm), which was rated to 0.1 N and had a resolution of 4 μN. This had the resolution needed, but required a method taking the data and using it with the displacement data from the tensile tester. At the time, we had planned on adding the signal as an external signal into the tensile tester. In order to find the size of the signal we would need to measure, we had to use the information from the load cell's data sheet. The load cell had a rated output of about 0.5 mV/V, and a maximum excitation voltage of 10 V. This meant that at the rated force of 0.1 N, there would be an output voltage of 5 mV. At the lowest measurable force of 4 μN, this would mean an output voltage of 200 nV. This small signal would need to be amplified in order to be used by the tensile tester. Alternatively, Novatech also sold a DCUSB load cell digitizer (https://www.novatechloadcells.co.uk/products/dscusb), which is a device for collecting data that paired with the load cell, but that could not connect directly to the tensile tester.

For the first option, we considered building a basic Op-Amp amplifier, and feeding the amplified signal into the tensile tester through a BNC plug, which the tensile testing software could synchronize with the displacement data automatically. The BNC plug that the tensile tester used had connected to an analog to digital converter with a 16 bit resolution, and a range of ±10 V. This means the lowest signal it could measure was approximately 300 μV, which would require our signal to be magnified by a factor of over 3000 to gain the full resolution of the load cell. Due to this large amplification, and the size of the input signals, low noise Op-Amps would be needed. We never settled on a specific Op-Amp, but from our research potential choices were the ADA4528 and the ADA8428, which both had noise levels that could have potentially worked.

For the second option, the DCUSB would have been able to measure the signal from the load cell and provide a force reading out of the box. However, there were two issues with this method. First, it only had a USB connection, meaning it would require a way to synchronize its force measurements with the tensile tester's displacement measurements. Second, using this device, the load cell's resolution would be 10 μN. We could have potentially improved this by averaging over multiple data points, however we were unable to come up with a method of synchronizing the data using this method, therefore we decided against this option.

Having settled on the F329 Deci-Newton load cell, we planned to order it over winter break to allow for the 5 week lead time. However, due to a lapse of communication at the end of the fall semester and over break, the order was not placed. Due to the long lead time, ordering at the beginning of the spring semester would have had it arriving around the end of February or beginning of March, which would not have

allowed enough time to perform tests with it. Fortunately, our mentor Professor Schniepp as well as a graduate student identified and ordered the 0.1N Ultra Low Capacity (ULC) Load Cell from Interface (https://www.interfaceforce.com/products/interface-mini/overload-protected/ulc-ultra-low-capacity-load-cell/). It is rated for a maximum axial overload of 1000% of its capacity, which is 1 N. This is lower than the threshold than the 1N load cell from MTS by almost an order of magnitude, reducing our margin of error for the mounting method.

Figure 5: ULC load cell with soldered D-sub connector.

As a suggestion from Professor Schniepp, we decided to pivot from attaching the load cell as an external signal and instead connect it directly into the existing load cell port. This approach allowed us to take advantage of the electronics inside the tensile tester, meaning we no longer had to build our own amplifier. The ULC load cell came with flying leads, or loose wires. It has five wires, which the company labels as +EXC, -OUT, -EXC, +OUT, and SHIELD, which correspond to points A, D, C, B on Figure 3, as well as a common ground. The load cells from the tensile tester connect using a 15 pin

D-sub port. Most of the 15 pins are either not used or not necessary, which allowed us to connect our ULC load cell by soldering the leads to a D-sub connector. We soldered the leads to a simple D-sub connector for the purposes of running tests and making sure that we had everything configured correctly, and planned on changing to a shielded connector once all of the settings were finalized. The only issue was that the tensile tester required a Transducer Electronic Data Sheet (TEDS) to work. A TEDS is essentially the data sheet for the load cell, but in a form the tensile tester can use. It contains what voltage inputs the load cell can take, the resistance of the bridge elements, the rated output, and other information. For the load cells from MTS, the TEDS was contained on a memory device inside the load cells and sent to the controlling software through two of the wires over the D-sub connector. After contacting MTS, they provided us with instructions for creating a virtual TEDS for the load cell in the tensile tester's software. We were able to fill in most of the information using the calibration sheet Interface provided with the load cell, however some values were not included, such as the response time or the specific Wheatstone bridge setup used. We put in placeholder information using assumptions from looking at TEDS signals for the MTS load cells, and contacted Interface to see if they could provide the remaining information. As of writing, however, they have not responded.

The MTS load cells came with spacers, which are needed to provide the necessary distance for the load cell to be unobstructed by the tensile tester itself when attaching the clamps for sample testing. The MTS load cell spacers are metal with female connectors that fit with the load cell's male connector. The 0.1N load cell was ordered from a different company, so the existing MTS metal spacers could not be used. A solid 3-D printed spacer (Figure 6a) was designed based on the MTS spacer dimensions. However, the design was modified to a hollow spacer (Figure 6b) because the solid spacer was too long for the screw which attaches the load cell to the tensile tester to go through. With the hollow spacer two screws can be used to separately attach the spacer to the tensile tester and the load cell to the spacer. Additionally the hollow spacer is a faster print, and reduces the amount of unnecessary filament needed to print.

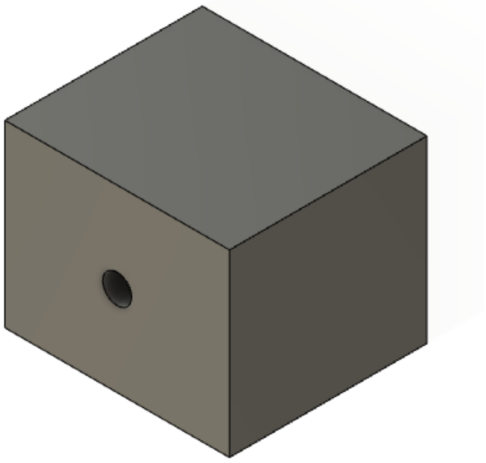

Figure 6a: Solid Spacer

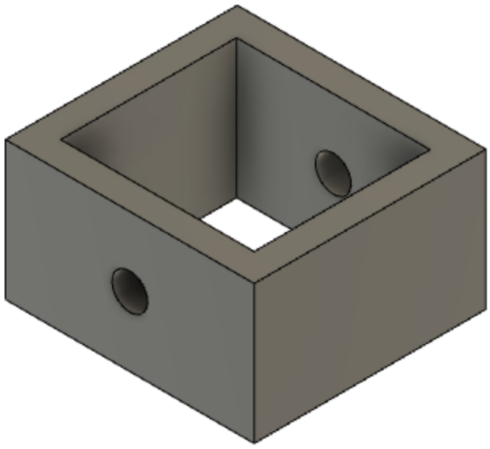

Figure 6b: Hollow Spacer.

3.2 Experimental Design

To begin initial testing on the fibers in question we needed a method that did not pre-strain the silk or introduce failure points when mounting, and that did not break the force sensors. The 1N load cell that comes with the tensile tester can handle up to 8 N before breaking, but the new load cell can only handle 1 N, requiring special precautions.

Before testing can begin we tackled the challenge of loading the fiber onto the mounts. For mounting fibers to the frame, we have tried several options, including Krazy Glues, Nail Polish, and Epoxy. We found Krazy Glue to be too wet, allowing the fibers to move too much before curing. We used Nail Polish because we wanted something more tacky, but it failed to hold the fibers properly. Finally, we moved to an epoxy that takes between 6 and 8 hours to set, and have found no further issues other than the long curing time.

The first mounting methods we considered were using a cardboard frame or a 3D printed frame. Other groups have used the cardboard frame, as the silk can be attached to the cardboard, and then the cardboard cut after the frame is mounted. We decided to use the 3D printed frame because it allowed us to modify the mount to suit our needs as we discovered them, and because the mounts are lightweight and uniform. The iterations of the 3D printed mount, as well as the reasons behind making newer iterations are shown below.

In order to not overload the sensor, the options we have considered were using magnets or compressed air. The magnet option was to attach a magnet to the load cell, and have an additional magnet that can be attached to the mounting frame. This allows for multiple mounts to be used without having direct contact to the load cell, reducing the potential for breaking it.

To test the fibers the mounts need to suspend samples while also being able to connect to the testing apparatus. The “Double L” design (Figure 7) addressed both of those requirements, but after testing this design we found that the two “L” shaped contact points needed more surface area for adhesion. Additionally, with the thought of this mount needing to be used on a 1N load cell we placed a cylindrical point at the top to be threaded so it would screw directly into the system. Unfortunately, the resolution of the print was too low for us to thread and confidently screw into the system without fear of it breaking off.

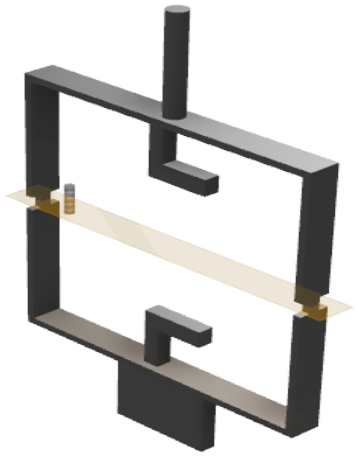

Figure 7: Double L Frame.

In the next design iteration we decided to focus on creating a mount that could be used with the 100N load cell. This design didn’t need a screw point since the top clamp could be used with the apparatus and not go overweight. With the “Double Plank” design (Figure 8) we addressed the problems from the previous design by elongating and widening the contact points and changed the cylindrical point to a flat piece to be clamped. After testing we found that the design worked perfectly for testing sheep’s wool, but if we want to move down to the 1N load cell we still needed to solve the top contact point issue.

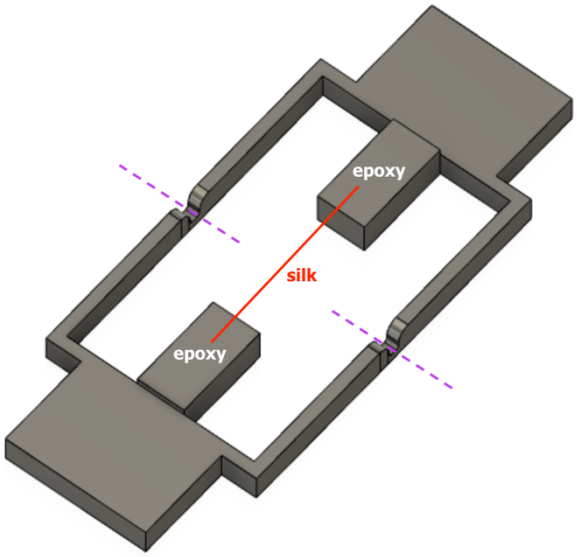

Figure 8: Double Plank Frame.

The next design iteration was called the “Screw Mount” (Figure 9) we again replaced the top clamp point, but instead of using a cylinder we made a space for a screw to go through to attach to the system. After testing we found that the physical load of screwing into the load cell as well as cutting the two breakpoints on the sides brought too much load unto the system.

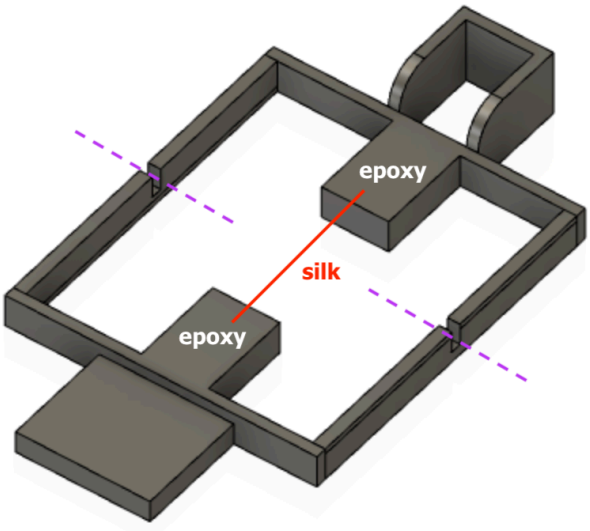

Figure 9: Screw Mount Frame.

The “Magna Screw” (Figure 10) removes the screw level from the previous iteration and replaces it with a magnet. We found that it would be easier to design a shelf for the magnet to rest on until the apparatus is attached to the machine. The “Magna Screw with Shelf” (Figure 11) was developed from this need. In this design, a screw with a magnet attached is directly screwed into the apparatus and magnet is placed on the level of the mount. This allows for the mount to seemingly self-attach bringing the mounting load down to almost zero. One breakpoint was removed and the other elongated to reduce the load being placed while cutting.

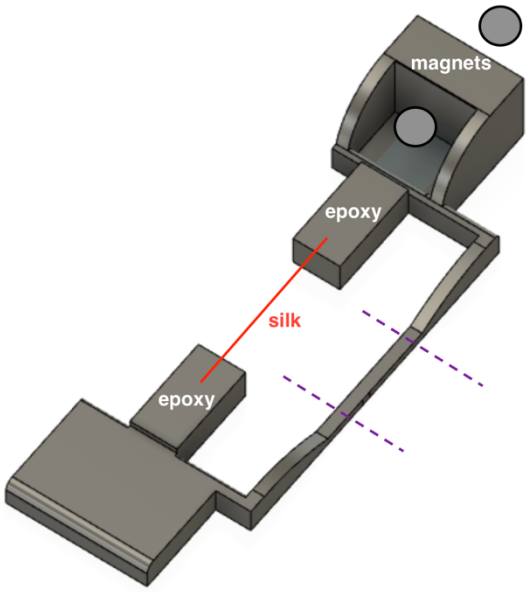

Figure 10: Magna Screw Mount Frame.

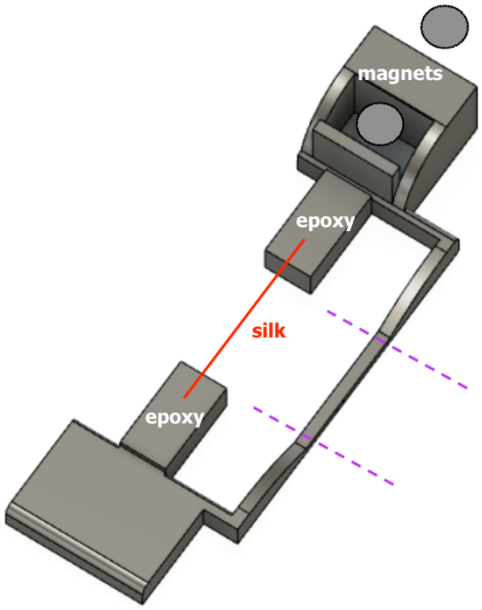

Figure 11: Magna Screw with Shelf Mount Frame.

The final iteration of the mount frames aimed to address how to connect our frames to the 0.1N load cell. The frame was designed to minimize load on the extremely delicate 0.1N load cell. The “Magna-T Frame” (see Figure 12a) features a Magnetic Mount that is attached to the load cell by the magnet placed in its shelf, which connects to the screw with a magnet that has been screwed into the load cell directly. The “T-bar” shape of the frame allows it to be carefully placed into the Tensile Tester without adding a load that will exceed the load cell’s capabilities.

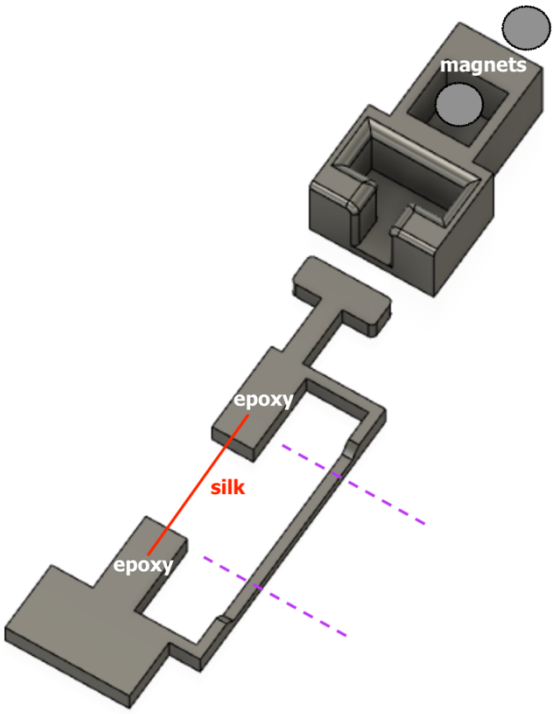

Figure 12a: Magna-T Frame with Magnetic Mount

4 Device Description

4.1 Status of the Apparatus

Currently, we have been able to connect the load cell to the tensile tester and receive a signal from it. However, this signal was incorrect by several orders of magnitude, measuring upwards of 15N when lying on the table. Additionally, at some point the tensile tester software began only showing errors when connected to the load cell. Due to the coronavirus situation, which impacted the last seven weeks of the semester, we have been unable to continue working in the lab to find the issues and finish integrating the load cell to the tensile tester.

4.2 Current Sample Mounting Implementation

The final iteration of the mounting frame is called the “Magna-T” frame (Fig. 12a, 12b), which combines aspects of previous frames. The frame which samples are mounted onto is detachable from the magnet mount. The magnet only has to be inserted into the mount once, and attached to the screw with an attached magnet that has already been screwed into the load cell. There is an increased amount of spacing between the magnet screwed into the load cell and the magnet in the magnet mount to account for load threshold.

Considering the 1N load cell's maximum load capacity of about 8N, we've taken delicate measures to assure our mounting technique does not overload the cell. To reduce the amount of force placed on the load cell we have developed a system of mounting a magnet upon a screw that is inserted into the load cell. Utilizing the Magna Mount, a magnet is placed in the upper space to allow for the magnet attached to the load cell to attract and "snap" into place without applying a disruptive load.

This sample mount was found to work best, having found no disadvantages at this time. Additionally, this process can also be used for a more precise load cell with a lower maximum load capacity. This is useful because when considering fibers that will snap quickly even with a load as small as 1N, this mounting technique can be used seamlessly while changing cells.

5 Device Application

5.1 Methods

Mounts were designed on Fusion 360 and printed using an Airwolf EVO 3D printer. Silk samples were prepared by first applying a layer of PC super epoxy onto the rectangular contact points of the mounting frames (as shown in Fig. 12b). An individual silk strand from the *B. mori* silkworm was isolated by gently using tweezers and tweezer scissors to cut to desired length. The loose strand of silk was placed on the contact points of the mount, making sure to not stretch the silk or get epoxy on the silk anywhere other than the contact points. Mounts were stored for 6 hours to allow epoxy to cure completely. Before running the tensile test, a magnet was first inserted into the holder and then attached to the load cell, and the T-bar of the mount was placed in the holder (as shown in Figure 12b). The adjustable clamp holding the bottom flat piece of the mount was tightened in order to make sure the mount was secure. Using a Kohree electric hot wire, the mount was cut at the breakpoints shown by the discontinuous lines in Fig. 12b. The tensile test on the individual silk strand was then run with an extension rate of 0.05 mm/s and raw data was collected. In order to compute the cross sectional area of the silk strands, the average diameter of the silk was determined by uploading an image taken on the Olympus microscope to the Image Viewer application on MATLAB. The width was measured in pixels and then converted to micrometers (as shown in Fig. 13).

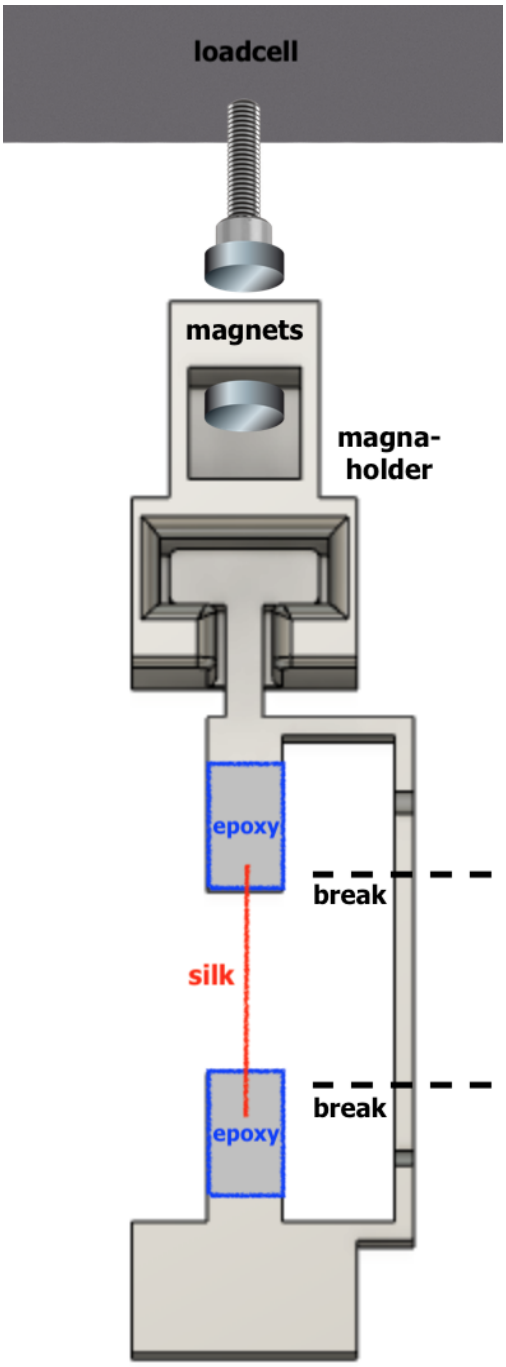

Figure 12b: Magna-T Frame with breakpoints at discontinuous lines

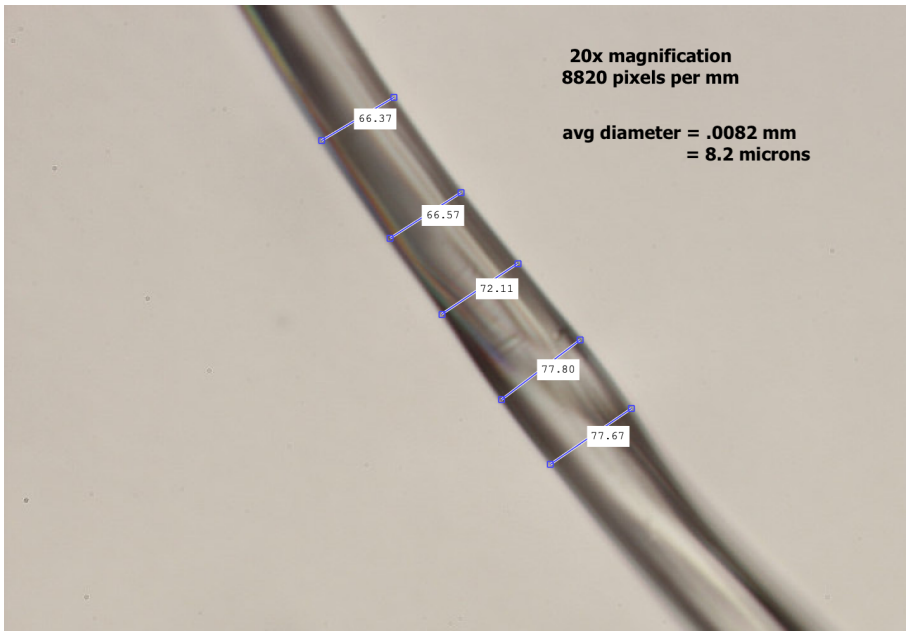

Figure 13: Image of B. mori silk taken on Olympus microscope

5.2 Results and Data Analysis from Silk Samples

Data Analysis

The data used for analysis came from strands of *B. mori* silk ran on the 1N load cell at 0.05 mm/s. The raw data starts out as a .txt file with 14 lines of useless data. In order to begin manipulating the data, the first 14 lines must be deleted. After this, the files are imported and converted into Excel files. From here the data is converted from text to numbers, and appropriate headers are added. The tensile machine records its data in “kN” and “mm”, which must be converted to “N” and “m” in order to later be calculated into stress vs strain.

Once the headers are properly named, the data is converted into readable numbers, and the units are scaled properly, the code is then able to be written to plot the data. The first set of plots for all 20 data sets are Force vs. Displacement plots. There are 4 different sections of code used in order to generate the plots. The first section locates the files and imports them into the studio. The second set of plots reads the data, finds its column headers and determines x and y coordinates. The third section scales the data to an appropriate portion so that it can be readable. The last section plots the data by assigning each data set with a specific color, assigns data labels and a data legend. The code is then executed and the plots are saved as PDF files.

After plotting all of the Force vs Displacement data, all of the datasets must then be converted to Stress vs Strain. First, the effective starting length must be calculated. The effective start length is the length at which the fiber strands have no more slack and a force begins to be read by the tensile machine. These values vary greatly between each test due to multiple different factors that will be discussed later in more detail. The data from the start length to the point at which the fiber breaks is the data to be used in the Stress vs Strain plots. The effective start length is subtracted by the break length to get the total displacement. With these values, the strain is able to be calculated using : $\boldsymbol{\varepsilon = dl / l_o}$ where $\boldsymbol{dl}$ is the change in length and $\boldsymbol{l_o}$ is the start length. The stress is then calculated by dividing force by cross-sectional area. The cross-sectional area of the silkworm fibers is calculated by taking the average radius of each sample. The stress and strain values are then combined into tables and multiplied together to calculate Young's Modulus $\boldsymbol{E}$.

The data is then converted into graphs using a similar process as above. The code for both of these sections is shown in Fig. 14a and Fig. 14b.

```
##TEST 1-5
#Load Data
mydata <- read.table("test1.ws.txt", sep = "\t", header = T)
mydata2 <- read.table("test2.ws.txt", sep = "\t", header = T)
mydata3 <- read.table("test3.ws.txt", sep = "\t", header = T)
mydata4 <- read.table("test4.ws.txt", sep = "\t", header = T)
mydata5 <- read.table("test5.ws.txt", sep = "\t", header = T)
#Reading/Scaling Data
mydata$Load.kN. <- mydata$Load.kN.*1000000
mydata2$Load.kN. <- mydata2$Load.kN.*1000000
mydata3$Load.kN. <- mydata3$Load.kN.*1000000
mydata4$Load.kN. <- mydata4$Load.kN.*1000000
mydata5$Load.kN. <- mydata5$Load.kN.*1000000
#Plotting Data
plot(mydata$Crosshead.mm., mydata$Load.kN., type = "l",
     xlab = "Distance (mm)", ylab = "Force (milliNetwons)", col = "darkgreen",lwd = 2,
     xlim = c(0, 12), main = "1N Silk Worm Tests 1-5",
     ylim = c(-5,80))
lines(mydata2$Crosshead.mm., mydata2$Load.kN., lwd = 2, col = "gold") # adding line for Test 2
lines(mydata3$Crosshead.mm., mydata3$Load.kN., lwd = 2, col = "lightblue")
lines(mydata4$Crosshead.mm., mydata4$Load.kN., lwd = 2, col = "blue")
lines(mydata5$Crosshead.mm., mydata5$Load.kN., lwd = 2, col = "purple")
legend("topright", legend = c("Test 1", "Test 2", "Test 3", "Test 4", "Test 5"), fill = c("darkgreen", "gold", "lightblue", "blue", "purple"))
```

Figure 14a: Force vs. Distance code.

```
#STRESS VS STRAIN DATA
# Load Data Section
##TEST 1-5
mydata <- read.table("ss1.tex", sep = "\t", header = F)
mydata2 <- read.table("ss2.tex", sep = "\t", header = F)
mydata3 <- read.table("ss3.tex", sep = "\t", header = F)
mydata4 <- read.table("ss4.tex", sep = "\t", header = F)
mydata5 <- read.table("ss5.tex", sep = "\t", header = F)
#Naming Columns
colnames(mydata) <- c("Strain", "Stress")
colnames(mydata2) <- c("Strain", "Stress")
colnames(mydata3) <- c("Strain", "Stress")
colnames(mydata4) <- c("Strain", "Stress")
colnames(mydata5) <- c("Strain", "Stress")
#plot data
plot(mydata$Strain, mydata$Stress, type = "l",
     xlab = "Strain", ylab = "Stress GPa", col = "darkgreen",lwd = 2,
     xlim = c(0, 3.5), main = "1N Silk Worm Tests 1-5 STRESS V STRAIN",
     ylim = c(0, 1.25))
lines(mydata2$Strain, mydata2$Stress, lwd = 2, col = "gold") # adding line for Test 2
lines(mydata3$Strain, mydata3$Stress, lwd = 2, col = "lightblue")
lines(mydata4$Strain, mydata4$Stress, lwd = 2, col = "blue")
lines(mydata5$Strain, mydata5$Stress, lwd = 2, col = "purple")
legend("topright", legend = c("Test 1", "Test 2", "Test 3", "Test 4", "Test 5"), fill = c("darkgreen", "gold", "lightblue", "blue", "purple"))
```

Figure 14b: Stress vs Strain code.

Force vs Displacement Data:

The force vs displacement data was split up into 5 tests each, totaling 4 separate plots. Each test is color coordinated, using a unique color for each test, but using that same color for the corresponding results in the stress vs strain curves in the later section. The force vs displacement plots are in millimeters and millinewtons. Millinewtons were used because they provided the most insight on the data, with values starting at 0 ± 0.024 mN and breaking between 40 ≅ 60 mN. The plots are shown in Figures 15 – 18.

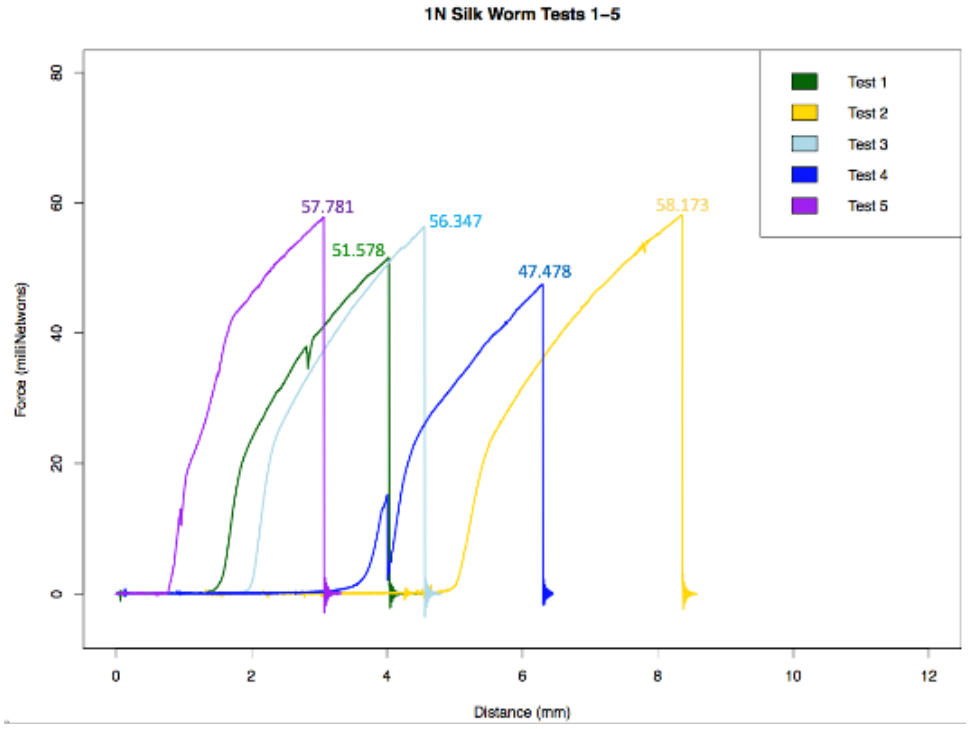

Figure 15: Force vs Displacement Plot Test 1-5.

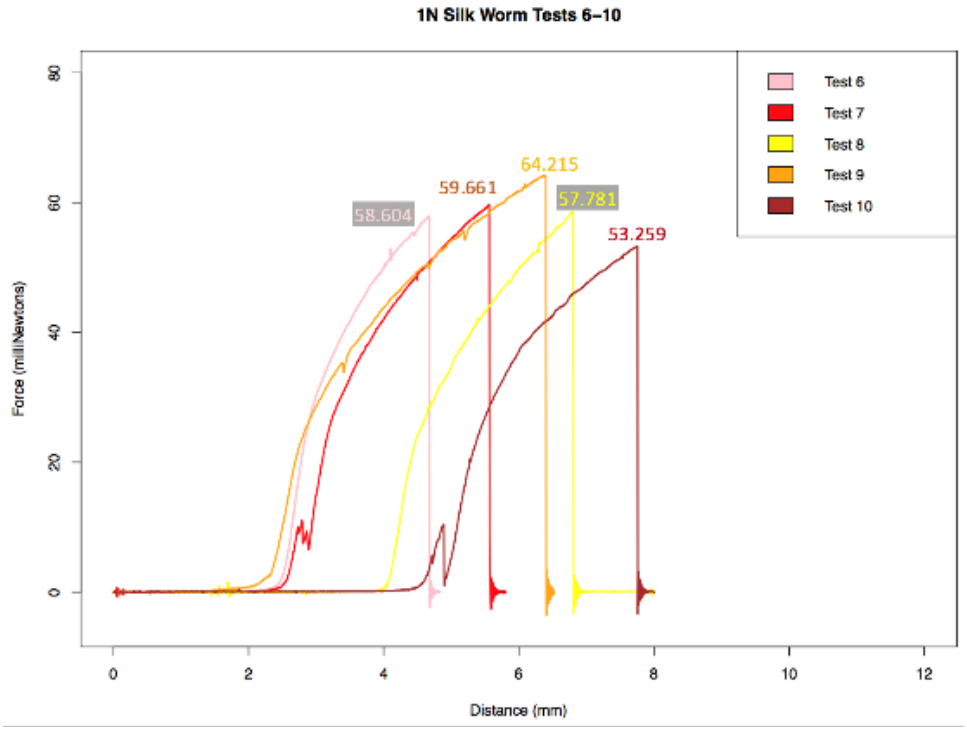

Figure 16: Force vs Displacement Plot Tests 6-10.

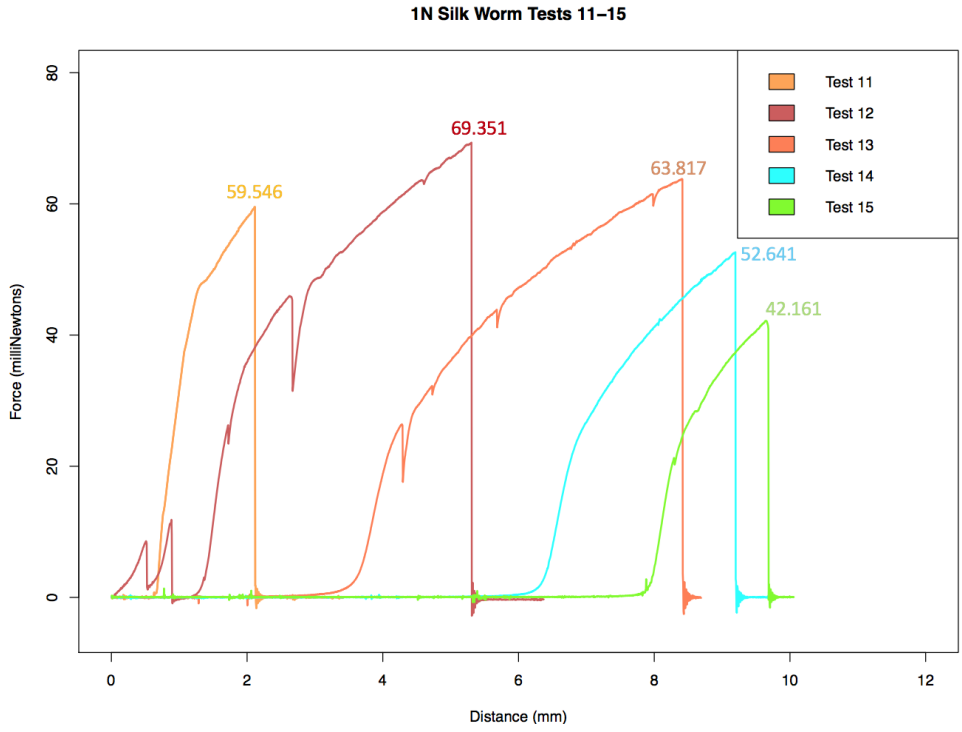

Figure 17: Force vs Displacement Plot Tests 11-15.

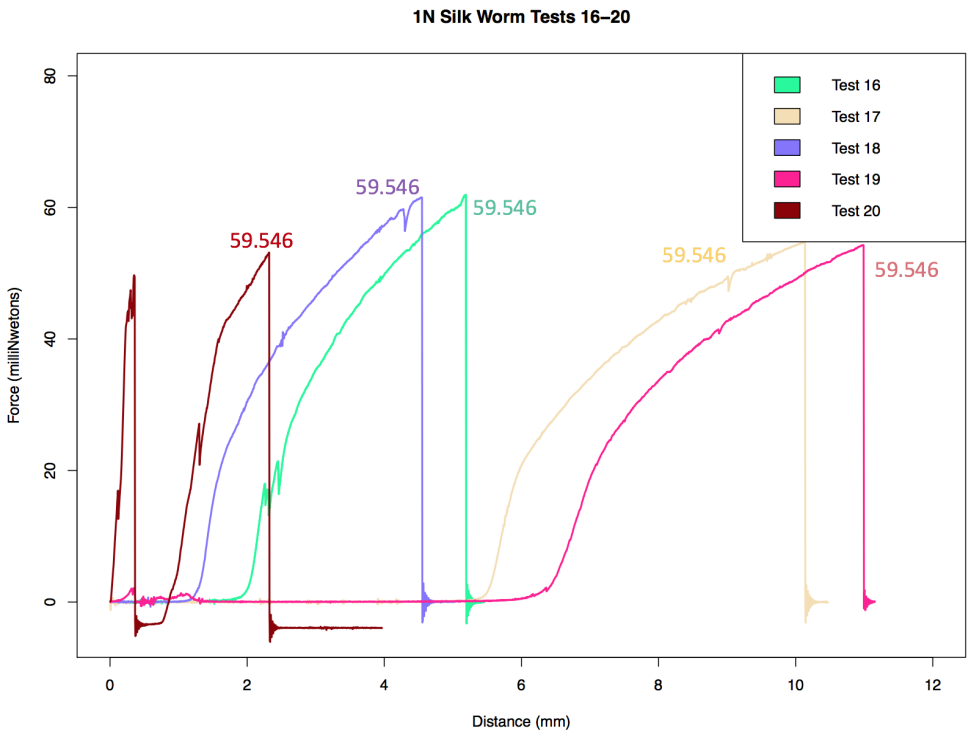

Figure 18: Force vs Displacement Plot Tests 16-20.

Max Force mN	
Test 1	51.578
Test 2	58.173
Test 3	56.347
Test 4	47.478
Test 5	57.781
Test 6	57.967
Test 7	59.661
Test 8	58.604
Test 9	64.215
Test 10	53.259
Test 11	59.546
Test 12	69.351
Test 13	63.817
Test 14	52.641
Test 15	42.161
Test 16	61.915
Test 17	54.785
Test 18	61.537
Test 19	54.282
Test 20	53.147
AVG	**56.912**
STD DEV	**6.137**

Table 1: Summary of Force vs Displacement.

Table 1 is a summary of all the tests max stress force applied before breaking, in millinewtons. The average breaking force is 56.912 mN ± 6.137.

Test	Start (mm)	Break (mm)	Total Dist (mm)	Force (N)
Test 1	1.2159	4.0356	2.8197	0.0516
Test 2	4.7953	8.3551	3.5598	0.0582
Test 3	1.7804	4.5557	2.7753	0.0563
Test 4	2.7658	6.3003	3.5345	0.0475
Test 5	0.7557	3.0657	2.3100	0.0578
Test 6	1.9617	4.6718	2.7101	0.0580
Test 7	2.1406	5.5609	3.4203	0.0597
Test 8	3.8209	6.8056	2.9848	0.0586
Test 9	1.4455	6.4004	4.9549	0.0642
Test 10	3.9858	7.7559	3.7701	0.0533
Test 11	0.6106	2.1158	1.5052	0.0595
Test 12	1.2005	5.3061	4.1056	0.0694
Test 13	2.6458	8.4154	5.7696	0.0638
Test 14	5.6958	9.1959	3.5002	0.0526
Test 15	7.5154	9.6813	2.1659	0.0422
Test 16	1.6557	5.1909	3.5352	0.0619
Test 17	5.1859	10.1358	4.9500	0.0548
Test 18	1.0909	4.5504	3.4595	0.0615
Test 19	5.6454	10.9902	5.3448	0.0543
Test 20	0.8559	2.3212	1.4653	0.0531
AVG			**3.4320**	**0.0569**
STD DEV			**1.1771**	**0.0061**

Table 2: Max Force Values

Table 2 summarizes the data for the Force vs Displacement graphs. The start length is the length at which the fiber started experiencing stress, the break length is where the fibers broke, the total distance traveled is the total length the fiber was under tension. The last column is the force converted to Newtons, which is to be used later on in the Stress vs Strain conversions.

Stress vs Strain Data

The effective start length varies greatly between tests for multiple reasons. When mounting the samples, there is a 10 mm gap that the silk is laid across. The silk is supposed to be glued with the least amount of slack possible, without actually applying any stretching force to it. This was found to be quite challenging, resulting in some samples to have upwards of 8 mm of slack. Other reasons for varying effective start lengths are slippages of the silk within the mounting epoxy. These are somewhat noticeable on some of the graphs, which will be discussed below. The last reason is due to the bracket mounting. The tensile tester is lowered into place, where the mount is then attached. When the mount is clamped it would often generate a little more slack. Though these cause major variations in the lengths and ultimately the force vs displacement plots, it does not affect the stress or strain results. The only factor that affects the outcome of the data is the displacement while under stress, which was proven to be precise to ± 0.005 mm. Below are the effective start/break length in meters, and the total distance stretched while under stress.

Test	Effective Start Length (m)	Effecttive Break Length (m)	ΔL (m)
Test 1	0.0112	0.0140	0.00282
Test 2	0.0148	0.0184	0.00356
Test 3	0.0118	0.0146	0.00278
Test 4	0.0128	0.0163	0.00353
Test 5	0.0108	0.0131	0.00231
Test 6	0.0120	0.0147	0.00271
Test 7	0.0121	0.0156	0.00342
Test 8	0.0138	0.0168	0.00298
Test 9	0.0114	0.0164	0.00495
Test 10	0.0140	0.0178	0.00377
Test 11	0.0106	0.0121	0.00151
Test 12	0.0112	0.0153	0.00411
Test 13	0.0126	0.0184	0.00577
Test 14	0.0157	0.0192	0.00350
Test 15	0.0175	0.0197	0.00217
Test 16	0.0117	0.0152	0.00354
Test 17	0.0152	0.0201	0.00495
Test 18	0.0111	0.0146	0.00346
Test 19	0.0156	0.0210	0.00534
Test 20	0.0109	0.0123	0.00147
AVG			**0.00343**
STD DEV			**0.00118**

Table 3: Effective Start/Break length and displacement.

Test	Strength (N)	Breaking Stress σ (GPa)	Breaking Strain Ɛ	Young's Modulus E (GPa)
Test 1	0.0516	0.9767	0.2514	16.742
Test 2	0.0582	1.1015	0.2406	20.038
Test 3	0.0563	1.0670	0.2356	12.824
Test 4	0.0475	0.8990	0.2769	9.815
Test 5	0.0578	1.0941	0.2148	9.424
Test 6	0.0580	1.0977	0.2266	4.079
Test 7	0.0597	1.1297	0.2817	8.455
Test 8	0.0586	1.1097	0.2160	32.352
Test 9	0.0642	1.2160	0.4329	4.852
Test 10	0.0533	1.0085	0.2696	5.870
Test 11	0.0595	1.1275	0.1419	9.584
Test 12	0.0694	1.3132	0.3666	14.376
Test 13	0.0638	1.2084	0.4562	3.181
Test 14	0.0526	0.9968	0.2230	9.742
Test 15	0.0422	0.7983	0.1237	14.092
Test 16	0.0619	1.1724	0.3033	9.893
Test 17	0.0548	1.0374	0.3260	6.889
Test 18	0.0615	1.1653	0.3119	9.339
Test 19	0.0543	1.0279	0.3416	11.193
Test 20	0.0531	1.0064	0.1350	11.003
AVG	**0.0569**	**1.0777**	**0.2688**	**11.187**
STD DEV	**0.0061**	**0.1162**	**0.0890**	**6.498**

Table 4: Stress vs Strain Data

STRESS VS STRAIN CURVES

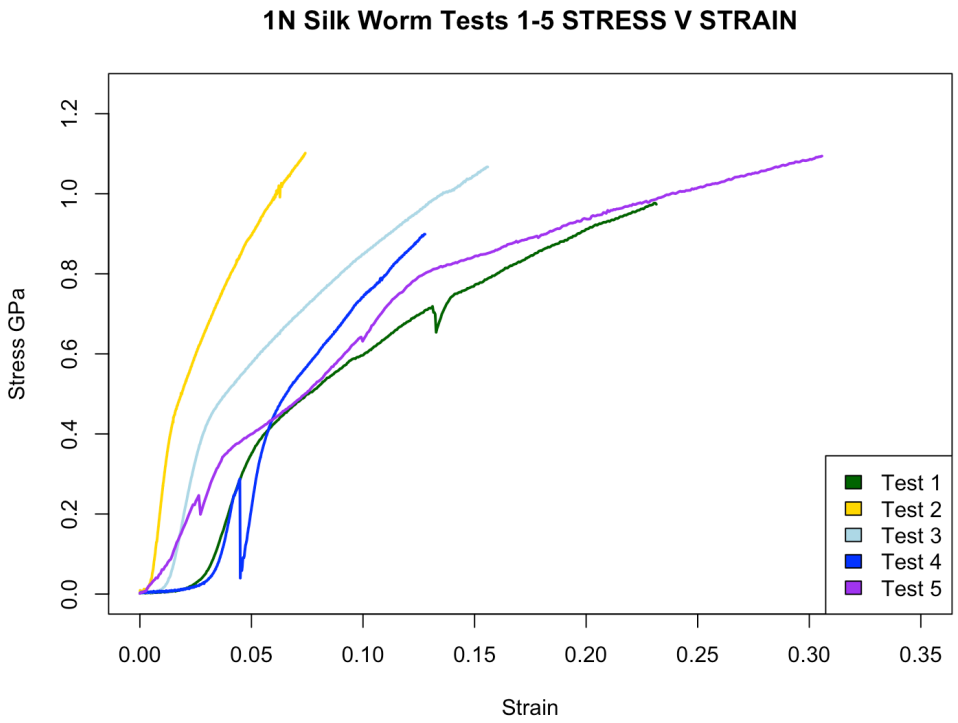

Figure 19: Stress vs Strain Plot Tests 1-5.

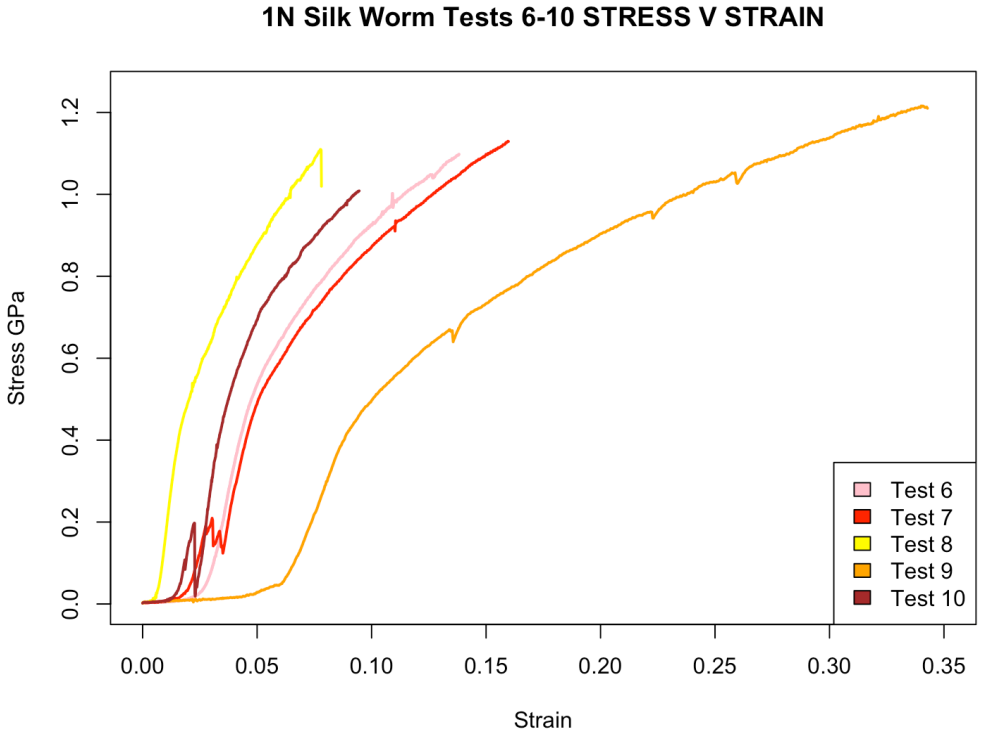

Figure 20: Stress vs Strain Plot Tests 6-10.

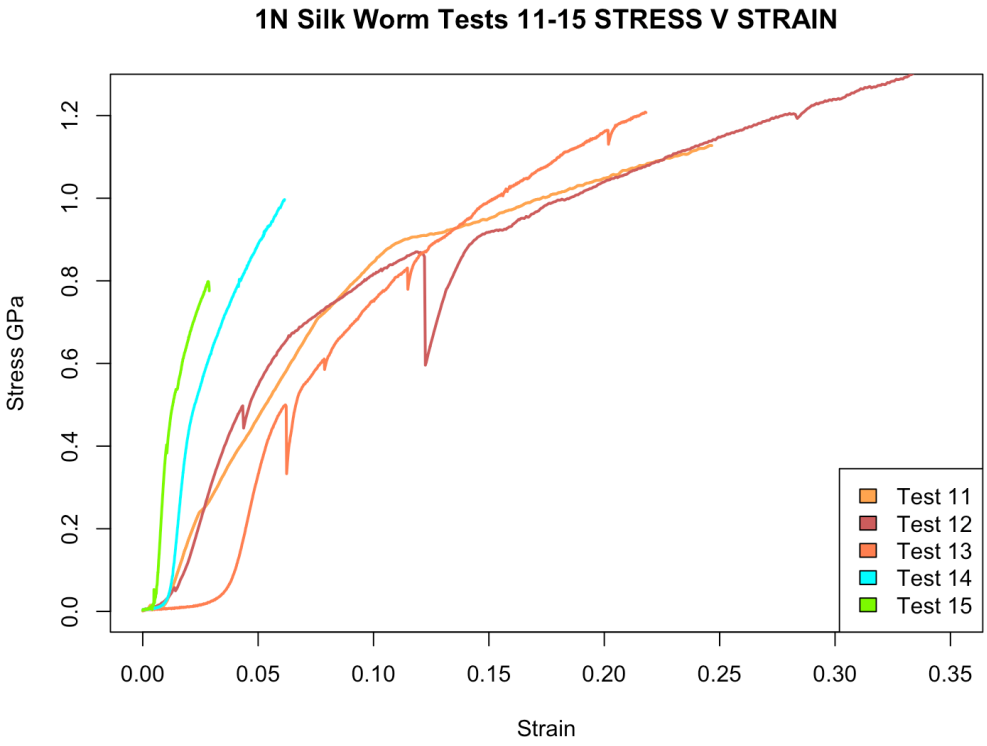

Figure 21: Stress vs Strain Plot Tests 11-15.

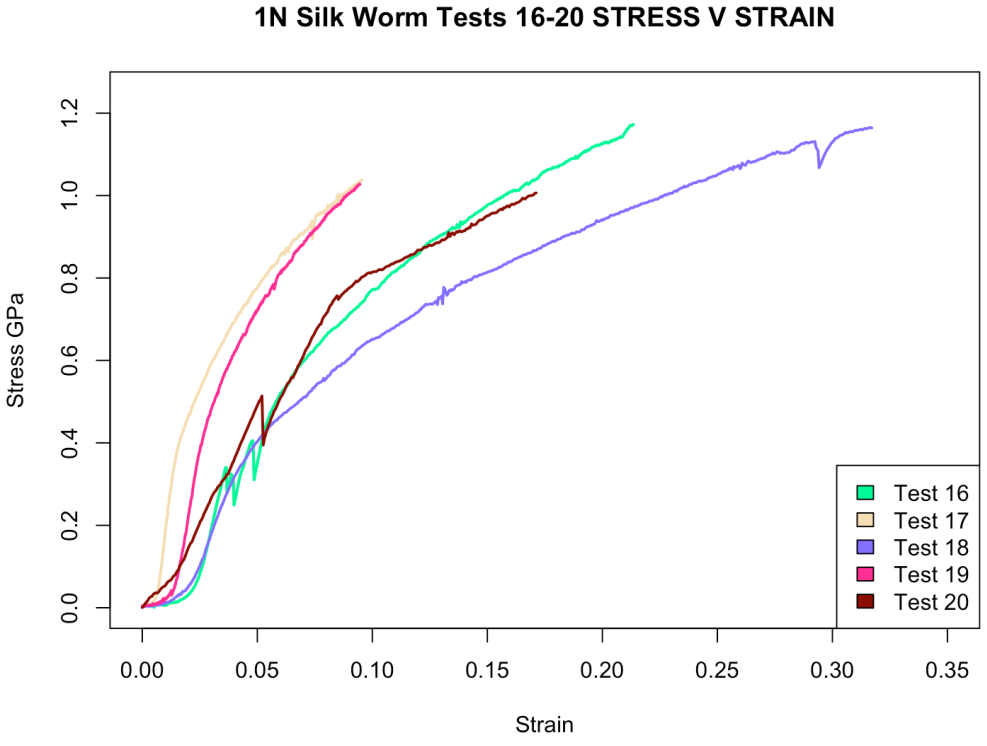

Figure 22: Stress vs Strain Plot Tests 16-20.

The force vs displacement graphs demonstrate prototypical behavior of worm silk under a tensile test. At the beginning there is a linear growth as force is applied to the silk representing the elastic region, and then a plastic region in the curve (beginning on average at 40 millinewtons) which demonstrates a permanent deformation in the silk. Average breaking point was 0.0569 N ± 0.0061 N (as shown in Table 4).

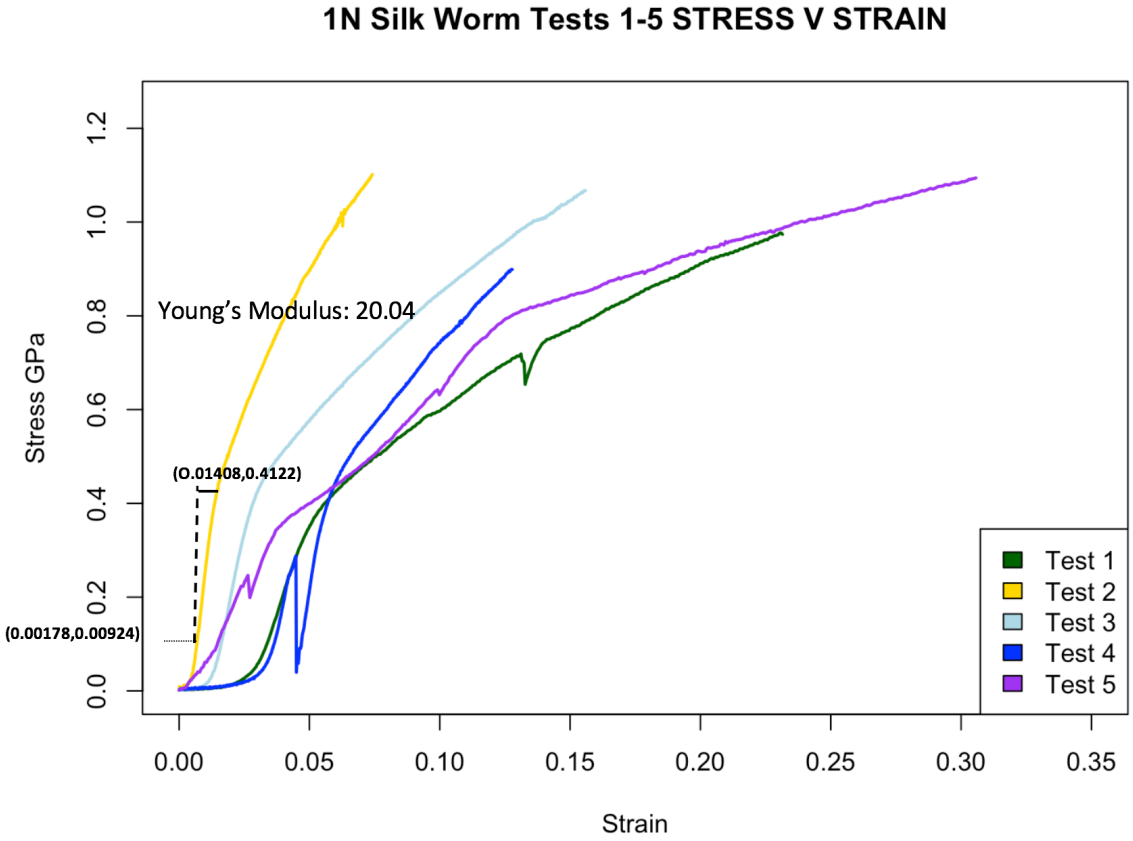

Figure 23: Young's Modulus Example for Test 2.

By taking the slope of the linear region of the stress-strain curve close to 0, we found an average young's modulus of 11.187 GPa ± 6.498 GPa. This is compared to the accepted modulus of *B. mori* silk of 7 GPa (Gosline et al. 1999). This silk has demonstrated a variability in experimental values across many groups (Chen et al 2019). The ranging differences in these Elastic Modulus values could potentially be explained by differences in cross-sectional area both within our experiment and from other groups. Another observation from the stress-strain curves produced was that they

visually behave like previous stress-strain examples of *B. mori* silk shown in Fig. 24 (P. Poza 2002).

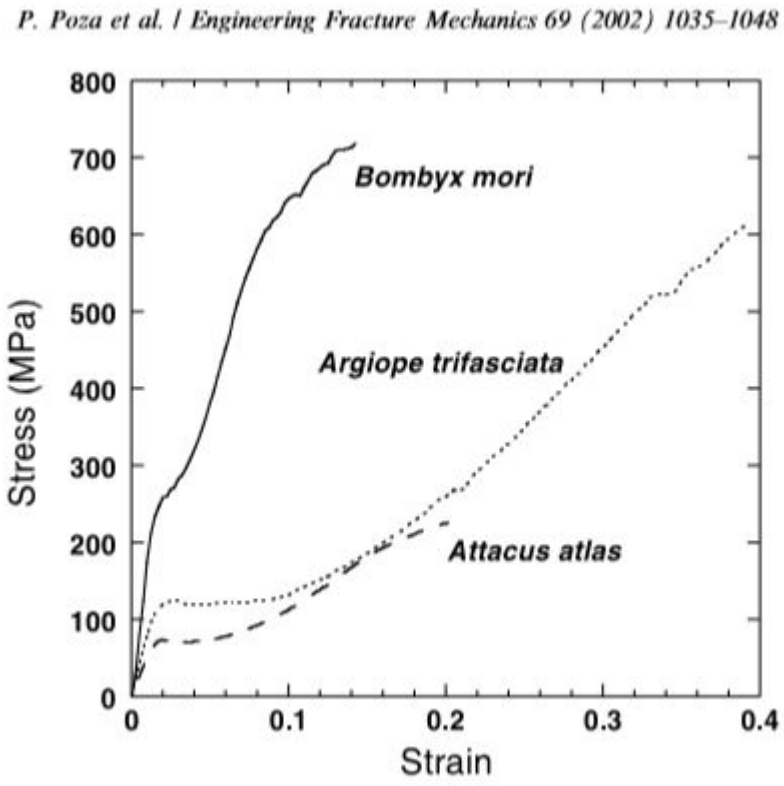

Figure 24: Stress Strain Curve of B. Mori Silk.

Additionally, what we see is evidence of ductility. Ductility is the physical property of a material which describes the material's ability to be drawn into a wire without fracturing (Helmenstine 2019). This is typically contrasted against the brittleness of a material, or the physical characteristic of a material that when subjected to stress fractures with little elastic or plastic deformation. The difference in the two can be demonstrated by Fig. 25.

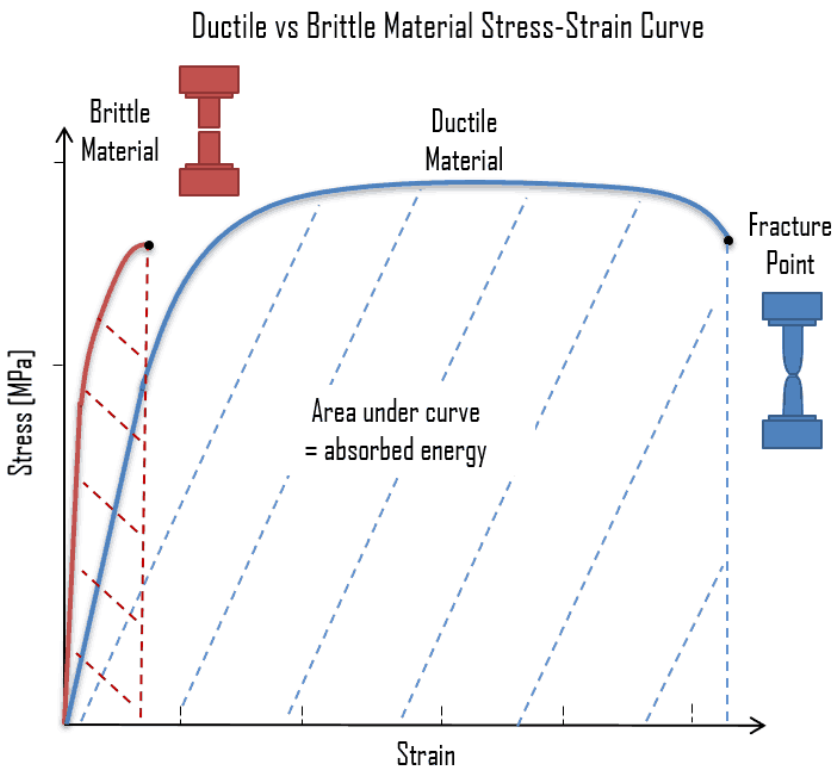

Figure 25: Image of Ductility vs Brittleness.

Our data and curves show that the *B. mori* silk is a ductile material, however it does have a shorter range of strain it can endure before fracture typically (compared to other more ultra-ductile silk) which is consistent with prior literature (P. Poza 2002). The behavior can be summarized as high strength and limited ductility.

Our graphs and data representations also show us errors in our project. We can identify slippage points on our curve where silk slipped during testing represented by the arrows in Fig. 26.

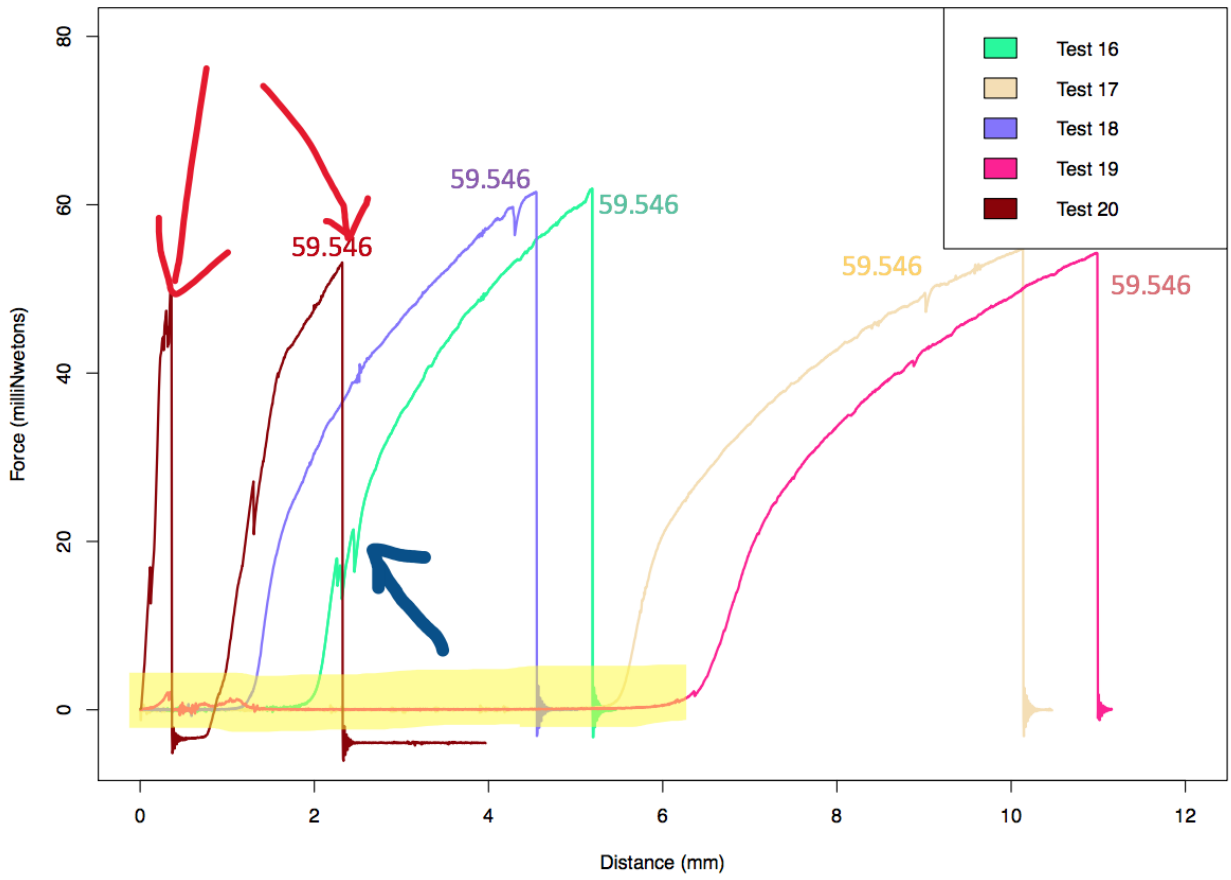

Figure 26: Annotations identifying noise.

There was slack in our silk samples, which is what lead to the varying start lengths demonstrated in Figure 18. This created inconsistencies in our tests that had to be manually corrected for by identifying an effective start length (on average 12.8 mm +/- 2.01) vs a perceived start length. True start length was intended to be 10 mm.

Finally, there was internal noise from the tensile tester described in section 5.3. These noise limits correspond with specific speeds:

- 0.1 mm/s had an average noise level of 32.16 μN with a standard deviation of 10.01
- 0.05 mm/s had an average noise level of 24.70 μN with a standard deviation of 3.27
- 0.01 mm/s had an average noise level of 19.26 μN with a standard deviation of 1.43

We chose 0.05 mm/s as a balance between noise level and expediency.

5.3 Device Performance

The noise levels were calculated by performing 5 tests with no force applied, providing an oscillation around 0. Each test ran for 1.5 mm, and then the standard deviation was taken of this data. The standard deviations of each test within each movement speed was then averaged out to provide the noise levels (as shown in Fig. 27).

.1mm/s	MicroNewtons
Test 1	23.314
Test 2	29.115
Test 3	49.185
Test 4	27.296
Test 5	31.906
AVG	**32.163**
STD DEV	**10.014**

0.05mm/s	MicroNewtons
Test 1	30.096
Test 2	22.867
Test 3	21.211
Test 4	22.588
Test 5	26.749
AVG	**24.702**
STD DEV	**3.266**

0.01mm/s	MicroNewtons
Test 1	17.649
Test 2	19.356
Test 3	20.613
Test 4	20.705
Test 5	17.965
AVG	**19.257**
STD DEV	**1.432**

Figure 27: Noise Levels

Due to the pandemic crisis preventing our debugging of the connection between the 0.1 N ULC Load Cell and the Criterion 42 tester, we were unable to follow the same process for the 0.1 N Load Cell. Our best option to predict experimental noise levels is thus to take the noise levels calculated from the 1 N load cell and divide them by a factor of 10. This would give the following values for the 0.1 N load cell:

- 0.1 mm/s had an average noise level of 3.22 μN with a standard deviation of 1.00
- 0.05 mm/s had an average noise level of 2.47 μN with a standard deviation of 0.33
- 0.01 mm/s had an average noise level of 1.93 μN with a standard deviation of 0.14

These values are promising, as the highest case of noise (at 0.1 mm/s) would be 3.22 μN with a standard deviation of 1.00. Referencing back to our desired specifications, our goal was to construct a device capable of operating at a magnitude of 3.0 μN. With our theoretical noise levels for the 0.1 N Load Cell we are successfully approaching the desired resolution.

6 Conclusion

Overall, we were able to deliver three separate pieces that we believe can be combined into a functional product with a small amount of fine tuning. First, we were able to connect the ULC load cell to the tensile tester both physically and electronically. Second, after many iterations, we have a method of mounting the silk fibers that reduces the chances of slipping or pre-straining the silk, and allows for multiple tests to be run without risking overloading the load cell during handling. Finally, we have a program that takes the force vs displacement data given by the tensile tester and converts it into a stress-strain curve, as well as calculating the Young's Modulus from each test. Unfortunately, we were unable to complete our initial goal of providing a fully functional setup to Professor Schniepp and his lab because of COVID-19 and the state-mandated closure of our labs and departure from campus. The remaining issue of the problems between the load cell and the tensile tester are likely able to be fixed by modifying the TEDS file, which can be done by further examining the information on the data sheet and through testing to find the incorrect values and vendor guidance.

Citations:

Afsar, Jalal. “Stress Strain Curve Explanation: Stages: Mild Steel.” Engineering Intro, 21 Nov. 2018, www.engineeringintro.com/mechanics-of-structures/stress-strain-curve-explanation/.

Chen, Shaoyong, et al. “Mechanical Properties of Bombyx Mori Silkworm Silk Fibre and Its Corresponding Silk Fibroin Filament: A Comparative Study.” *Materials & Design*, Elsevier, 31 July 2019, www.sciencedirect.com/science/article/pii/S0264127519305155.

Daley, Jason. “Brown Recluse Silk Is Stronger Than Steel Because It's Constructed Like a Cable.” Smithsonian.com, Smithsonian Institution, 21 Nov. 2018, www.smithsonianmag.com/smart-news/brown-recluse-silk-made-cable-180970871/.

Glover, Simon. “Simon Glover.” Ecotextile News, www.ecotextile.com/2019091725038/materials-production-news/scientists-combine-spider-silk-and-wood-to-replace-plastic.html.

Gosline, J. M., et al. “The Mechanical Design of Spider Silks: From Fibroin Sequence to Mechanical Function.” *The Journal of Experimental Biology*, 1999, biomimetic.pbworks.com/f/The+mechanical+design+of+spiderGosline.pdf.

Helmenstine, Anne Marie. “What Does Ductile Mean?” *ThoughtCo*, ThoughtCo, 16 Sept. 2019, www.thoughtco.com/definition-of-ductile-and-examples-605051.

Ko, Frank, et al. “Engineering Properties Of Spider Silk.” Web.mit.edu, 2018, web.mit.edu/3.064/www/slides/Ko_spider_silk.pdf.

Lee, Kevin. “What Are the Effects of Non-Biodegradable Waste?” Sciencing, 2 Mar. 2019, sciencing.com/effects-nonbiodegradable-waste-8452084.html.

MiceliNov, Courtney. “Spider Silk Is Five Times Stronger than Steel-Now, Scientists Know Why.” Science, 26 Dec. 2018, www.sciencemag.org/news/2018/11/spider-silk-five-times-stronger-steel-now-scientists-know-why#.

Pérez-Rigueiro, J., et al. “Tensile Properties Of Argiope Trifasciata drag Line Silk Obtained from the Spiders Web.” Journal of Applied Polymer Science, vol. 82, no. 9, 2001, pp. 2245–2251., doi:10.1002/app.2072.

Pool, Rebecca. “Sustainable Polymers: Plastics with Potential.” RSS, 13 Mar. 2019, eandt.theiet.org/content/articles/2019/03/sustainable-polymers-plastics-with-potential/.

Poza, P., et al. *Fractographic Analysis of Silkworm and Spider Silk*. 2002, citeseerx.ist.psu.edu/viewdoc/download?doi=10.1.1.582.2195&rep=rep1&type=pdf.

Römer, Lin, and Thomas Scheibel. “The Elaborate Structure of Spider Silk: Structure and Function of a Natural High Performance Fiber.” Prion, Landes Bioscience, 2008, www.ncbi.nlm.nih.gov/pmc/articles/PMC2658765/.

Schniepp, Hannes C., et al. “Brown Recluse Spiders Nanometer Scale Ribbons of Stiff Extensible Silk.” Advanced Materials, vol. 25, no. 48, Aug. 2013, pp. 7028–7032., doi:10.1002/adma.201302740.

Shankman, Sabrina, and Paul Horn. “The Most Powerful Evidence Climate Scientists Have of Global Warming.” InsideClimate News, 7 Mar. 2019, insideclimatenews.org/news/03102017/infographic-ocean-heat-powerful-climate-change-evidence-global-warming?gclid=EAIaIQobChMIgLfDtvn16AIVkYzICh276QJKEAAYASAAEgIGrPD_BwE.

Wang, Qijue, and Hannes Schniepp. “Strength of Recluse Spider's Silk Originates from Nanofibrils.” ACS Macro Letters, 2018, pubs.acs.org/doi/10.1021/acsmacrolett.8b00678.